



Preliminary Report on Assessment of Environmentally-Assisted Fatigue for LWR Extended Service Conditions

S. Mohanty, W. K. Soppet, S. Majumdar, and K. Natesan

Nuclear Engineering Division
Argonne National Laboratory

March 2013

Nuclear Engineering Division

About Argonne National Laboratory

Argonne is a U.S. Department of Energy laboratory managed by UChicago Argonne, LLC under contract DE-AC02-06CH11357. The Laboratory's main facility is outside Chicago, at 9700 South Cass Avenue, Argonne, Illinois 60439. For information about Argonne, see www.anl.gov.

Disclaimer

This report was prepared as an account of work sponsored by an agency of the United States Government. Neither the United States Government nor any agency thereof, nor UChicago Argonne, LLC, nor any of their employees or officers, makes any warranty, express or implied, or assumes any legal liability or responsibility for the accuracy, completeness, or usefulness of any information, apparatus, product, or process disclosed, or represents that its use would not infringe privately owned rights. Reference herein to any specific commercial product, process, or service by trade name, trademark, manufacturer, or otherwise, does not necessarily constitute or imply its endorsement, recommendation, or favoring by the United States Government or any agency thereof. The views and opinions of document authors expressed herein do not necessarily state or reflect those of the United States Government or any agency thereof, Argonne National Laboratory, or UChicago Argonne, LLC.

Preliminary Report on Assessment of Environmentally-Assisted Fatigue for LWR Extended Service Conditions

S. Mohanty, W. K. Soppet, S. Majumdar, and K. Natesan

Nuclear Engineering Division
Argonne National Laboratory

March 2013

This page intentionally left blank

ABBREVIATIONS

ANL	Argonne National Laboratory
ASME	American Society of Mechanical Engineers
BWR	Boiling Water Reactor
COD	Crack Opening Displacement
DOF	Degree of Freedom
EAC	Environmentally Assisted Cracking
FEM	Finite Element Method
GFEM	Generalized Finite Element Method
ID	Inner Diameter
LOCA	Loss of Coolant Accident
LWR	Light Water Reactor
MAXPS	Maximum Principal Stress
NRC	Nuclear Regulatory Commission
OD	Outer Diameter
ORNL	Oak Ridge National Laboratory
PUM	Partition of Unity Method
PWR	Pressurized Water Reactor
RCS	Reactor Coolant System
RT	Room Temperature
SCC	Stress Corrosion Cracking
SICC	Strain Induced Corrosion Cracking
SG	Steam Generator
SS	Stainless Steel
UTS	Ultimate Tensile Strength
XFEM	Extended Finite Element Method

ACKNOWLEDGEMENTS

This research was sponsored by the U.S. Department of Energy, Office of Nuclear Energy, for the Light Water Reactor Sustainability Research and Development effort, under the program manager Dr. Jeremy Busby.

1 Introduction

Under the light water reactor sustainability (LWRS) program, the following two major activities are being conducted at Argonne National Laboratory:

- a) Mechanistic modeling of environmental fatigue
- b) Environmental tensile and/or fatigue testing on base, similar and dissimilar metal welds.

The completed and planned environmental testing activities are summarized below. It is to be noted that a detailed status report describing the results of the work performed under both mechanistic modeling and environmental fatigue testing will be submitted in the near future.

LWRS test activities completed or planned for completion include

- Base metal tensile test under room temperature.
- Two room temperature tensile tests of 316 base metal specimens. The two tests were conducted at different strain rates - 0.0001/s and 0.001/s in order to establish strain rate dependency of the material and to aid in subsequent finite element model development.
- Base metal fatigue test at room temperature
Two strain-controlled room-temperature fatigue tests of 316 base metals have been completed. Both tests were conducted at a strain rate of 0.001/s and with a strain amplitude of 0.005 (0.5 %) in order to verify the repeatability of the test setup and material behavior. Two more fatigue tests at different strain amplitudes planned for near future.

2 Room Temperature Tensile Testing of 316 Stainless Steel Base Metal

2.1 Introduction

Room-temperature tensile tests are needed for both 316 SS and 508 LCS base materials in order to establish the base line material behavior, such as stress-strain curve, yield stress, ultimate stress, etc. Based on these baseline behaviors, the test parameters for room temperature fatigue and subsequently the parameters for environmental fatigue tests will be determined. In addition, these room temperature material properties can be used for mechanistic modeling through finite element simulation. To date, the room-temperature tensile tests have been completed only for 316 SS which is the base metal for all weldments in our study, as is discussed in details in the following subsections. Tests were conducted at two strain rates, a slower rate of 0.0001 /S (0.01% /S) and a faster rate of 0.001 /S (0.1% /S). Note that, although the room-temperature tensile material properties of 316 SS are available in the literature, they may not be representative of the particular heat and material composition of the ANL fatigue specimens.

2.2 Heat information and material composition of 316 SS base metal

The 316 SS specimens used in the current work were fabricated from 316 SS plate stored in the ANL's material repository. The plate was originally procured from Eastern Stainless Company (currently closed) in 1979. As described by the manufacturer, the plate was water quenched and mill annealed at 1900 °F. The heat number for the material is P91576 and the corresponding chemical composition is given in Table 1.

Table 1.1: Chemical composition of Type 316 SS base metal

	Chemical composition %									
Heat No.	C	CR	CU	MN	MO	N	NI	P	S	SI
P91576	0.21	17.37	0.2	1.64	2.12	0.067	10.77	0.018	0.010	0.46

2.3 Test specimen

Hourglass specimens conforming to ASTM standard E8/E8M [1] and E606 [2] have been fabricated for both tensile and fatigue testing of the base metal. The specimens were fabricated along the rolling direction of a 316 SS plate as shown in Figure 1.1. The detail dimensions of the specimen are given in Figure 1.2. Figure 1.3 shows a picture of the as-fabricated specimen.

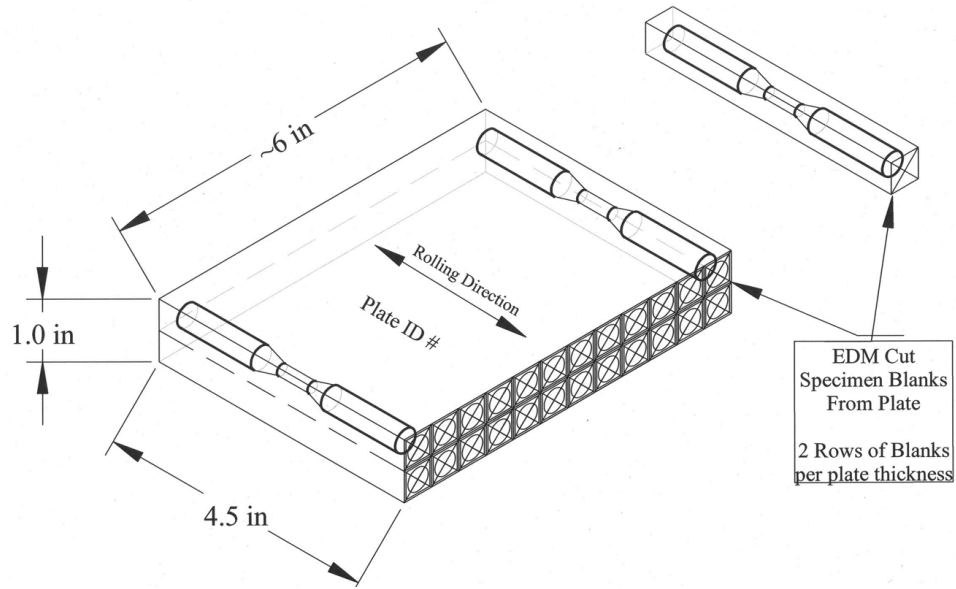


Figure 1.1. Hourglass specimen cutting plane with respect to plate rolling direction

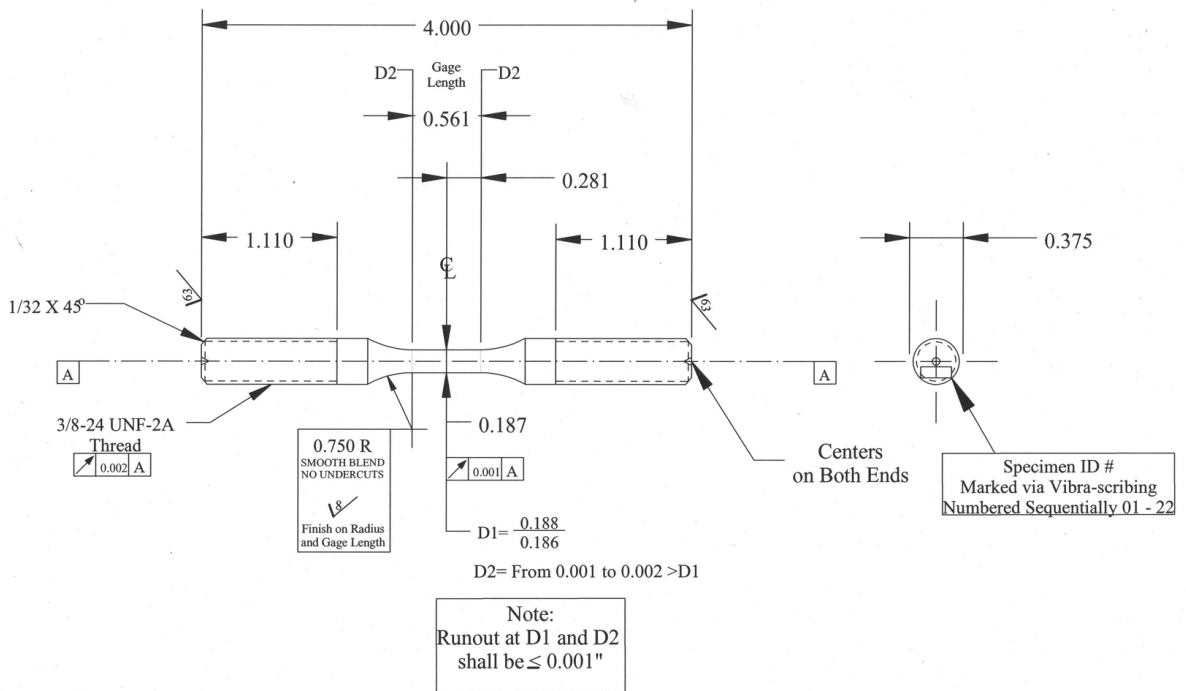


Figure 1.2. Geometry of the 316 SS tensile/fatigue specimen



Figure 1.3. Image of the fabricated 316 SS tensile/fatigue specimen

2.4 Experimental setup

A hydraulic controlled MTS test frame was used for the tensile and fatigue tests described in this report. The test frame with the installed specimen is instrumented to measure various test related parameters, as seen in Figure 1.4. In general, data measurements were collected by the following built-in or added-on sensors:

- a) Built-in test frame load cell
- b) Built-in test frame actuator position sensor for actuator position measurement
- c) Added-on displacement (stroke) sensor for crosshead position measurement
- d) Added-on extensometer for strain measurement
- e) Added-on in-house built ultrasonic sensor system for online/real-time structural health monitoring

It is to be noted that for the current in-air tests, extensometer based strain signal is used as feedback to control the axial strain of the test specimens. However, for environmental testing it may not be feasible to insert the extensometer into the test chamber and the controller feedback has to be obtained from either the test-frame built-in actuator position sensor or added-on crosshead displacement sensor that can be mounted outside the environmental chamber. A different test frame with environmental chamber is currently being configured at ANL's low cycle fatigue laboratory for future use in the LWRS-related environmental fatigue tests.

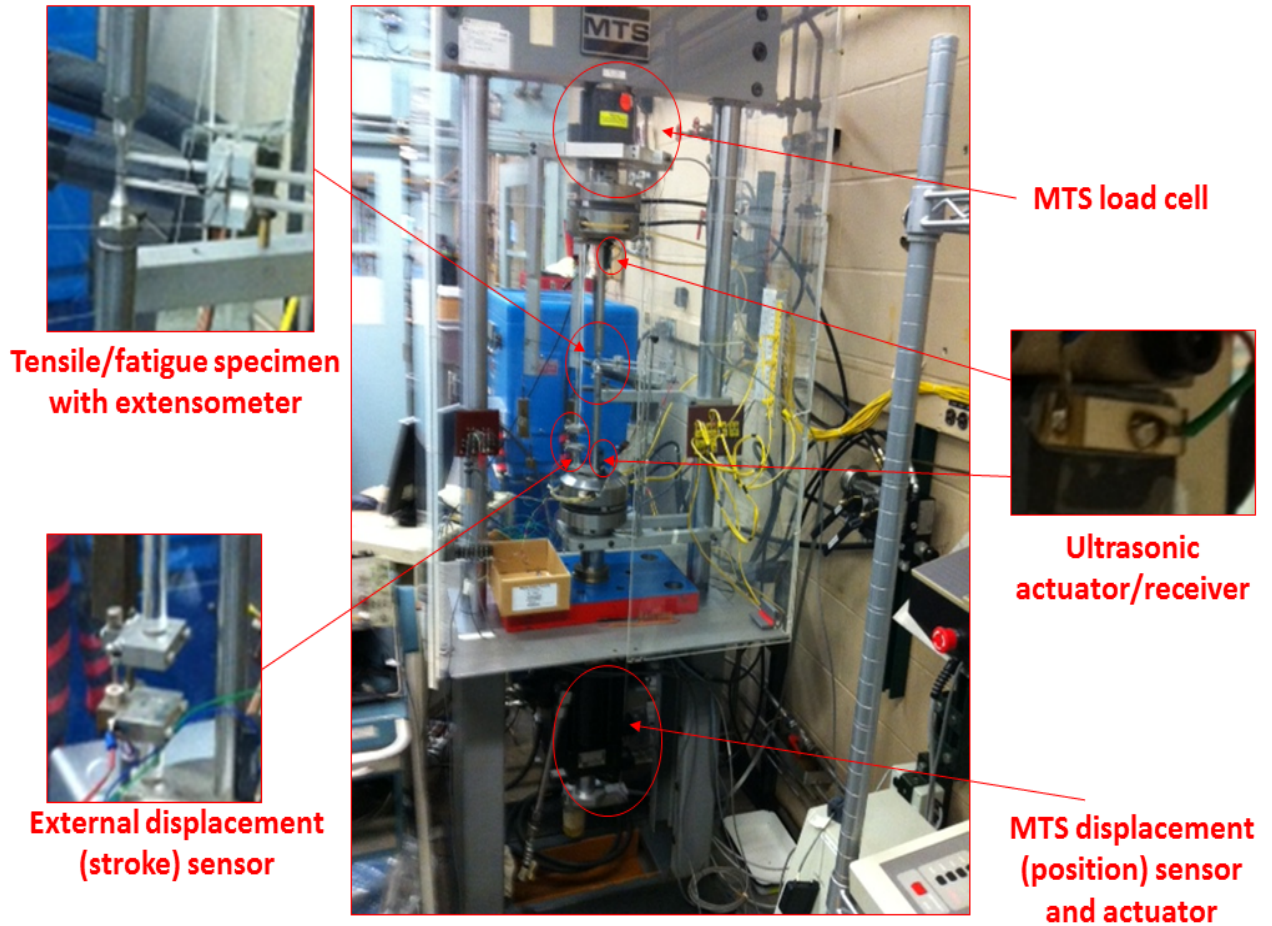


Figure 1.4. In-air tensile/fatigue test frame with specimen and various instruments

2.5 Tensile test results

Two tensile tests were conducted in air at room-temperature on Type 316 SS specimens. The tests were conducted at two different strain rates: a slower rate of 0.0001 /S (0.01% /S) and a faster rate of 0.001 /S (0.1% /S). The details of the test results are described below.

2.5.1 Stress-strain curve based on extensometer and load cell measurements

The estimated stress-strain curve using extensometer and load cell signal is shown in Figure 1.5. A strain-rate-dependent hardening effect is evident in Fig. 1.5. The faster strain rate test specimen experienced higher stress than the test specimen tested at a slower strain rate. This rate-dependency of the stress evident in tensile tests has to be included in fatigue modeling. Also, these stress-strain curves provide the elastic modulus and yield stress. The estimated elastic moduli and 0.2 % offset yield stresses for strain rates of 0.0001 /S and 0.001 /S are schematically shown in Figure 1.6 and 1.7, respectively. Because of the limits of the extensometer-design, Figures 1.5-1.7 show the maximum strains up to 2 %. The same extensometer will be used for elevated temperature tensile and fatigue testing. This is not a serious constraint for the fatigue

tests, which will generally have axial strain amplitudes $\leq 1\%$. The strain measurement capability of the available extensometer may be more limited during elevated temperature fatigue testing .

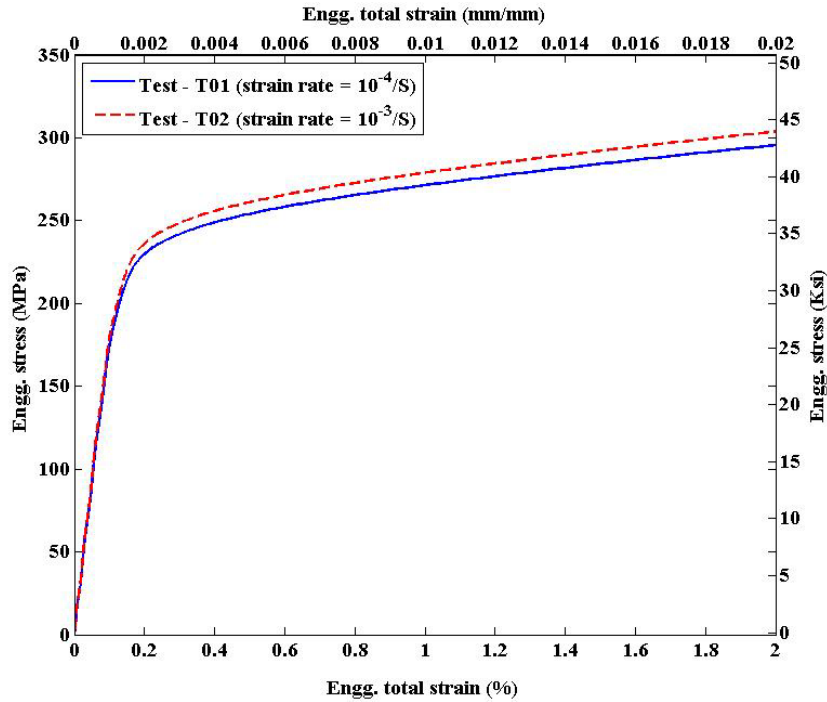


Figure 1.5: Strain versus stress plot estimated from measurements of extensometer and load cell

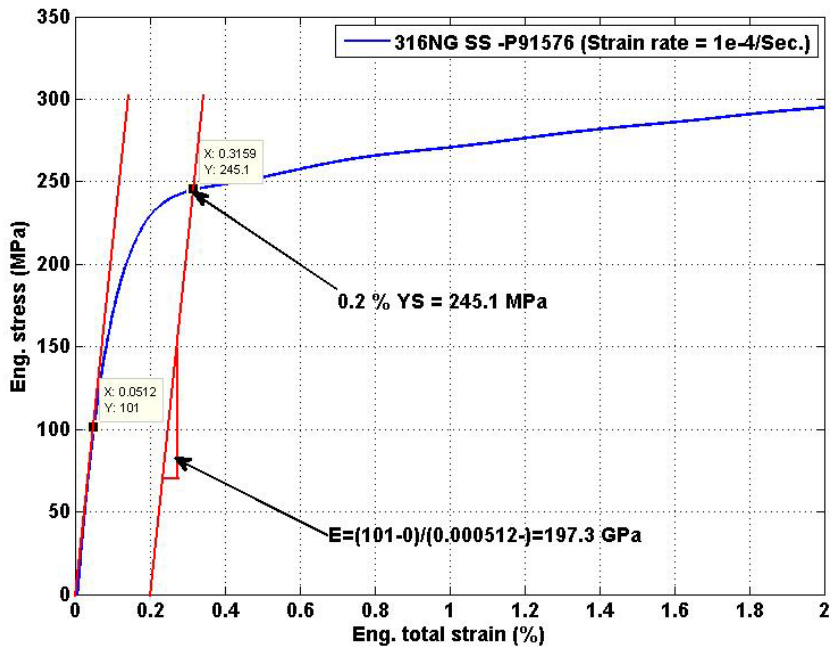


Figure 1.6: Strain versus stress plot showing estimated elastic modulus and 0.2% offset yield stress for

0.0001/S strain rate tensile test

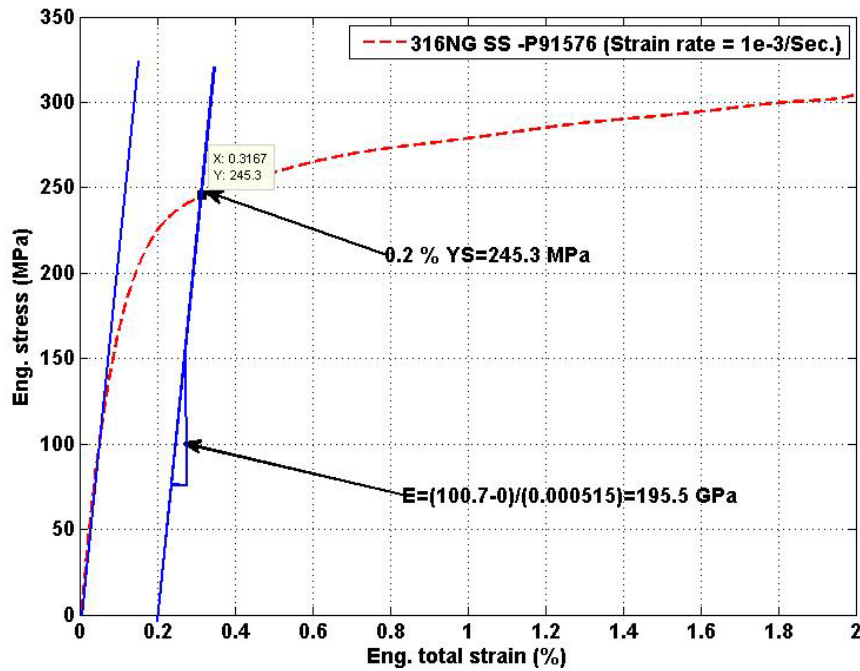


Figure 1.7: Strain versus stress plot showing estimated elastic modulus and 0.2% offset yield stress for 0.001/S strain rate tensile test

2.5.2 Stress-strain curve based on actuator/crosshead position and load cell measurements

As mentioned earlier, the extensometer used in the test has a maximum strain amplitude of 2 %. Although this limit is adequate for strain-control fatigue testing, it may not be sufficient for use in finite element modeling, in which the locally accumulated plastic strain may exceed 2%. The higher strain limit stress-strain curve can be estimated using the measured displacements from added-on crosshead position (stroke) sensor or using test frame actuator position sensor. The original displacements versus stress curve corresponding to crosshead position and actuator position sensor measurements are shown in Figure 1.8 and 1.9, respectively. Comparing Fig. 1.9 with Fig. 1.8 it can be seen that the crosshead displacement sensor has a more limited range. This is due to the use of a ceramic displacement sensor, which has a limited measurement range of 0.635 mm (0.025 inch). It is to be noted that both the extensometer and the crosshead displacement sensor can work under elevated temperature environment and will be used for the future in-air elevated temperature tensile/fatigue testing. However, unlike the extensometer, which cannot be inserted inside an environmental chamber for environmental fatigue testing, the crosshead position sensor is located outside the environmental chamber and will be used along with a calibration curve to control the axial strain in the specimen in the future during environmental fatigue testing.

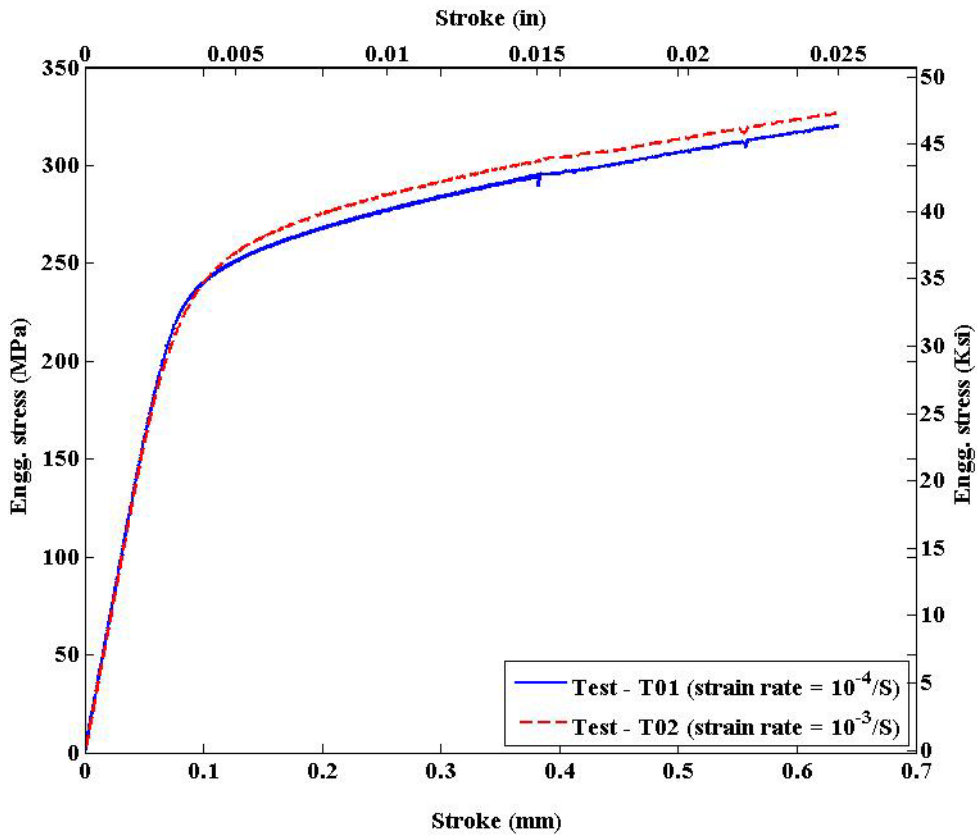


Figure 1.8: Crosshead displacement (stroke) versus stress plot

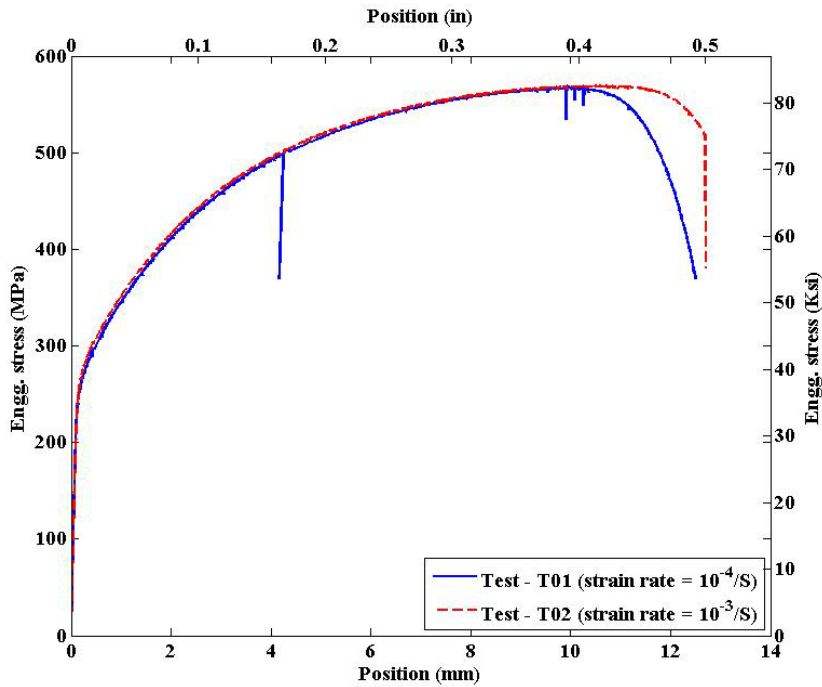


Figure 1.9: Actuator position versus stress plot

Figures 1.8 and 1.9 show the measured stress as a function of displacement. For finite element analysis input, it is necessary to convert these load-displacement curves to equivalent stress-strain curves. It is also necessary to estimate the equivalent strain from measured displacement for deciding test parameters in a strain-control fatigue test where extensometer cannot be used. This estimation can be performed by mapping known displacement to known strain and then predicting unknown strains from the known displacements. For simplicity a mapping function can be established between known displacements with known strain through least square fit. Using the estimated parameters of the mapping function the unknown strain can be estimated from the known or measured displacements. The known strain at a given instant of time ϵ_t can be expressed as

$$\epsilon_t = \frac{l_t - l_o}{L_{eff}} = \left(\frac{1}{L_{eff}}\right)l_t + \left(\frac{-l_o}{L_{eff}}\right) \quad (1.1)$$

Where l_t is the known or measured displacement at time t , l_o is the initial displacement, L_{eff} is the effective gage length and $\frac{1}{L_{eff}}$ and $\frac{-l_o}{L_{eff}}$ are the unknown parameters those can be estimated through least square fit. The comparison of crosshead displacement (stroke) and actuator position with respect to known strain can be seen from Figure 1.10 and 1.11, respectively.

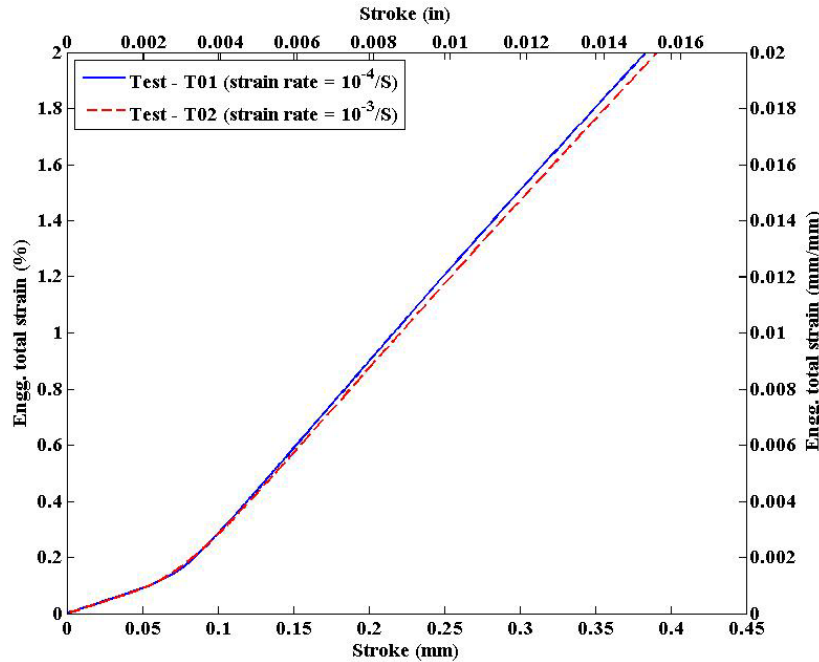


Figure 1.10: Crosshead displacement (stroke) with respect to known strain

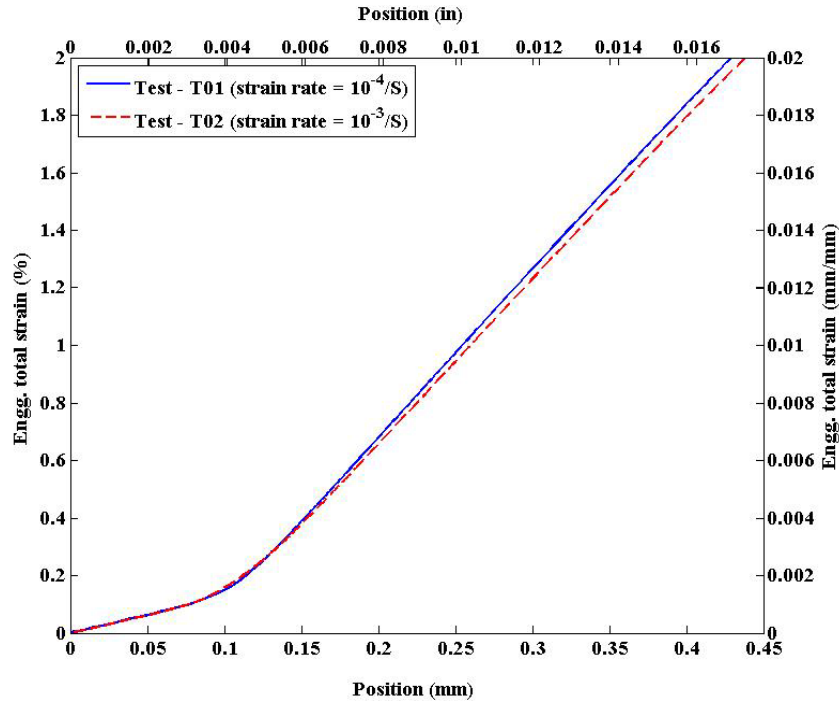


Figure 1.11: Actuator position with respect to known strain

Using Eq. 1.1 and the known crosshead and actuator position data shown in Figure 1.10 and 1.11, the effective length L_{eff} can be estimated. To note that for estimating the least square fit parameter the straight portion of the curve (shown in Fig. 1.10 and 11) i.e the position/stroke ~ strain data beyond the yield strain are only considered. The comparison of estimated L_{eff} and the physical gage length is given in Table 1.2. The corresponding estimated strain versus stress curve with respect to crosshead and actuator position measurements are shown in Figures 1.12 and 1.13 respectively. In addition, a summary of the scalar material properties estimated from the above-mentioned tensile test data and results can be found in table 1.3.

Table 1.2: Estimated effective gage length compared to specimen nominal gage length

Specimen No. (Strain rate)	Crosshead displacement based estimated L_{eff} in mm (in)	Actuator displacement based estimated L_{eff} in mm (in)	Specimen nominal gage length
1 (0.0001/S)	16.507 (0.649)	17.272 (0.68)	14.25 (0.561)
2 (0.001/S)	16.842 (0.663)	17.268 (0.68)	14.25 (0.561)

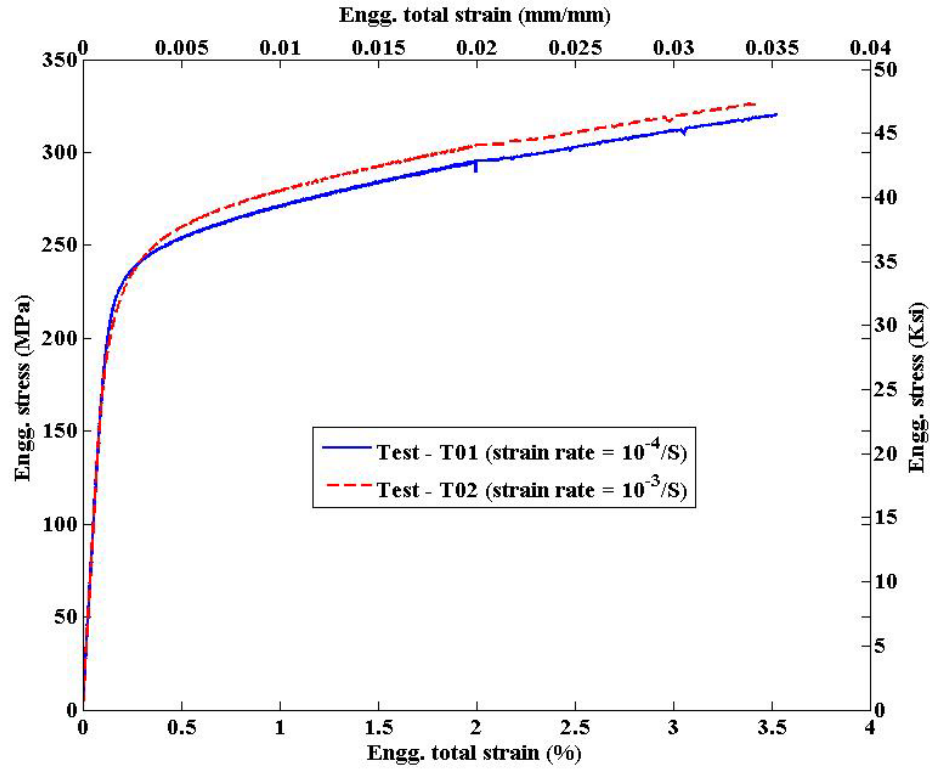


Figure 1.12: Strain versus stress curve estimated with respect to crosshead displacement measurements

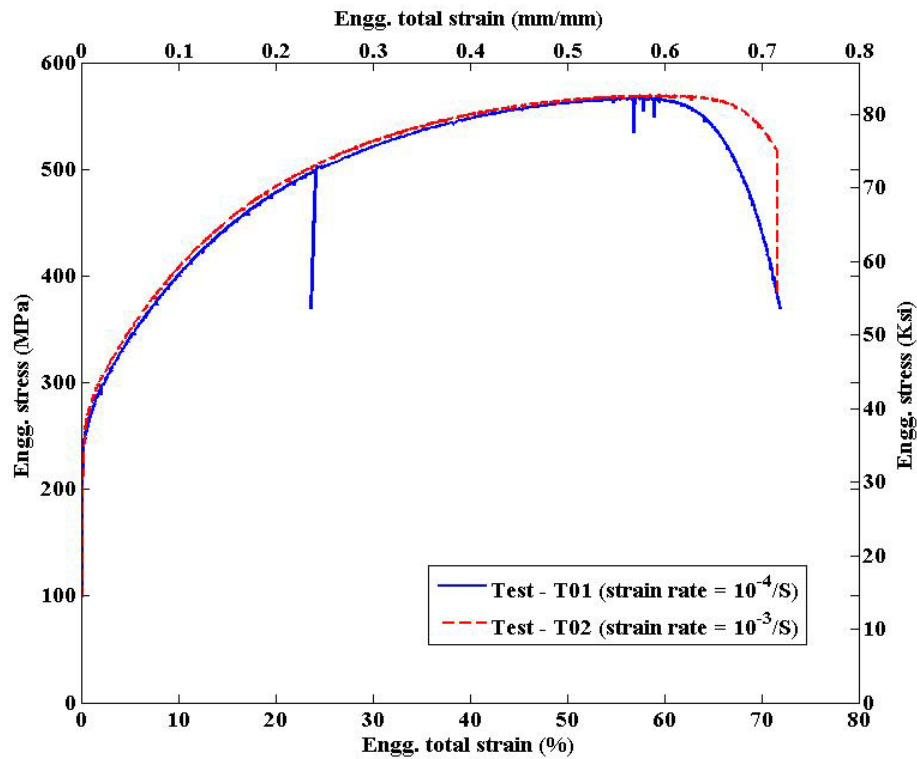


Figure 1.13: Strain versus stress curve estimated with respect to actuator position measurements

Table 1.3: Estimated room-temperature material properties of 316 SS base metal

Test number	Elastic modulus in GPa (Ksi)	0.2 % yield stress in MPa (Ksi)	Ultimate stress in MPa (Ksi)	Fracture stress in MPa (Ksi)	Fracture strain (%)	Reduction in gage area (%)
T01 (strain rate = 0.0001 /S)	197.3 (28615.9)	245.1 (35.55)	568.9 (82.51)	369.5 (53.59)	71.88	84.4
T02 (strain rate = 0.001 /S)	195.5 (28354.9)	245.3 (35.58)	569.1 (82.54)	380.5 (55.18)	71.57	83.1

2.6 Conclusion

Room temperature tensile tests of 316 SS base metal have been conducted under two strain rates: 0.0001 /S and 0.001/S. Based on these tensile test data room temperature material properties and stress-strain curves are estimated. These test results are or will be used in finite element based mechanistic modeling and for deciding test parameters for LWRS program related fatigue testing.

3 Summary of ongoing tasks

The ongoing effort on other subtasks is summarized below.

3.1 Room temperature fatigue testing of 316 SS base metal

As one of the subtasks under activities 316 SS base metal will be fatigue tested under room-temperature and in-air condition to estimate the base-line strain (stress)-life curve. All these tests are strain controlled fatigue tests. Also from these test results the baseline strain ratcheting behavior and hardening parameter will be estimated. A total of 5-6 tests are planned with different strain amplitudes. To date two specimens have been fatigue tested both under a strain amplitude of 0.5 % and strain rate of 0.001 /S (0.1 %/S). Figure 2.1 shows some typical example of hysteresis plot estimated using extensometer based strain and load cell measurements. This figure shows the initial stress hardening and then softening of the material.

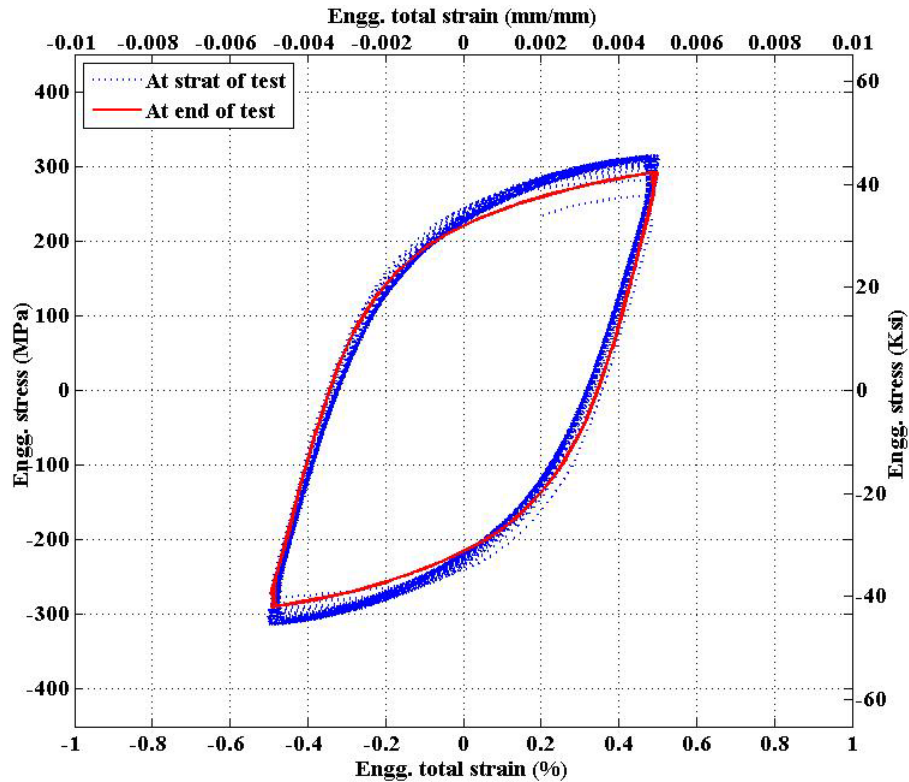


Figure 2.1: Comparison of extensometer measurement based hysteresis plot at the start and end of test

3.2 Mechanistic modeling of room temperature fatigue of 316 SS base metal

One of the subtasks of mechanistic based environmental fatigue modeling work has been initiated first to the model the room temperature fatigue using finite element model. The aim of this exercise is not only to estimate the fatigue life of material under room temperature condition but also to develop finite element model that can be representative enough to capture the real physical behaviors such as strain ratcheting, softening, hardening, etc. Figure 2.2 shows the typical finite element model of the tested 316 SS base metal specimen. Also Figure 2.3 shows the example of estimated hysteresis plot from this preliminary FEA using the isotropic hardening model.

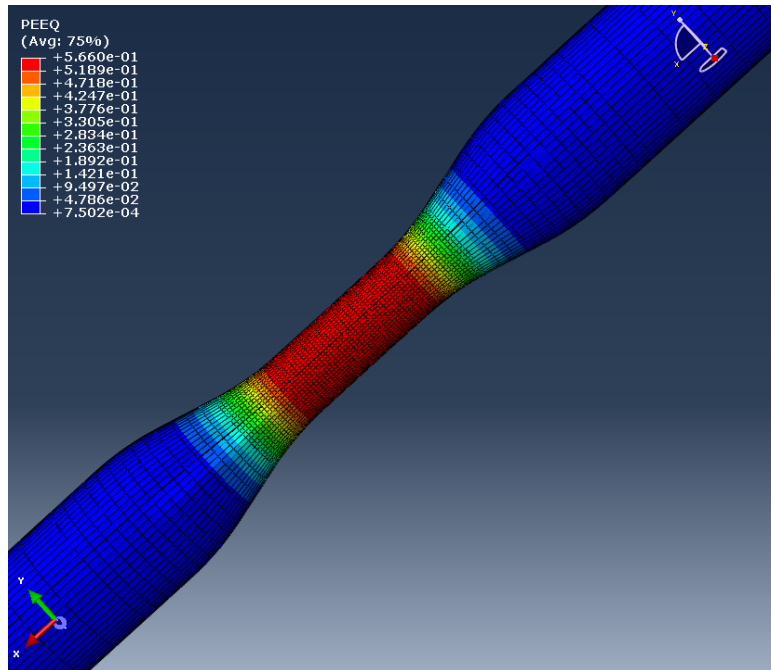


Figure 2.2: Finite element model of the 316 SS specimen with showing preliminary results of accumulated effective plastic strain (absolute scale) field distribution

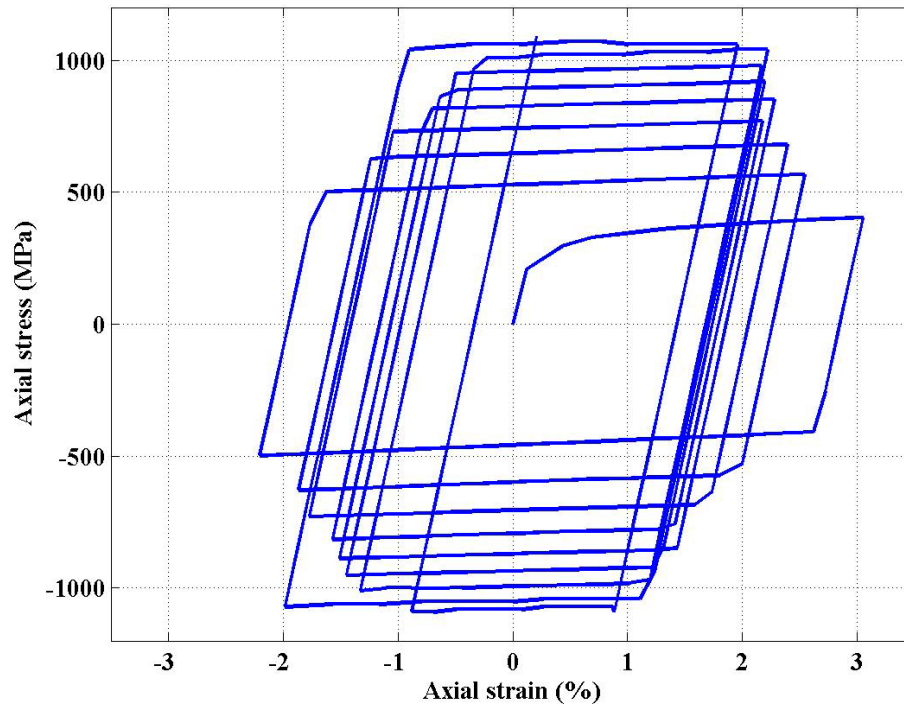


Figure 2.3: Hysteresis plot estimated from the preliminary finite element model showing stress hardening

3.3 Similar metal weld (316 SS – 316 SS) plate and specimen fabrication

As one of the experimental subtasks the fabrication of 316SS-316SS base metal specimen is under progress. Figure 2.4 shows the top view of the section of the welded plates whereas Figure 2.5 shows the cross section of the plate including the V-weld shape. Using these welded plates, multiple specimens are being fabricated either along or across the heat-affected zone of the weld.



Figure 2.4: Image showing top-view of the 316 SS-316 SS welded plate



Figure 2.5: Image showing cross-section of the 316 SS-316 SS welded plate

3.4 Similar metal weld residual stress characterization and modeling

Significant residual stresses can be generated during the welding process. These stresses may lead to stress corrosion cracking under the influence of LWR environment. In developing mechanistic models, the effects of these residual stresses need to be included. Figure 2.6 shows a typical example of residual stress distribution at the weld cross-section. These residual stresses were measured for the 316SS-316SS similar metal weld plate, using X-ray diffraction techniques by Lambda Research Inc at Cincinnati, Ohio. From the figure it can be seen that there is substantial compressive residual stress at the center of weld and tensile stress at the bottom of the weld. Comparing this results with the stress-strain curve shown in Figure 1.5 and assuming that the elastic properties of base metals holds good in the heat affected zone it can be shown that the residual strain is well above the 0.2 % offset yield strain. These preliminary results suggest that proper care has to be taken of residual stresses in developing mechanistic models.

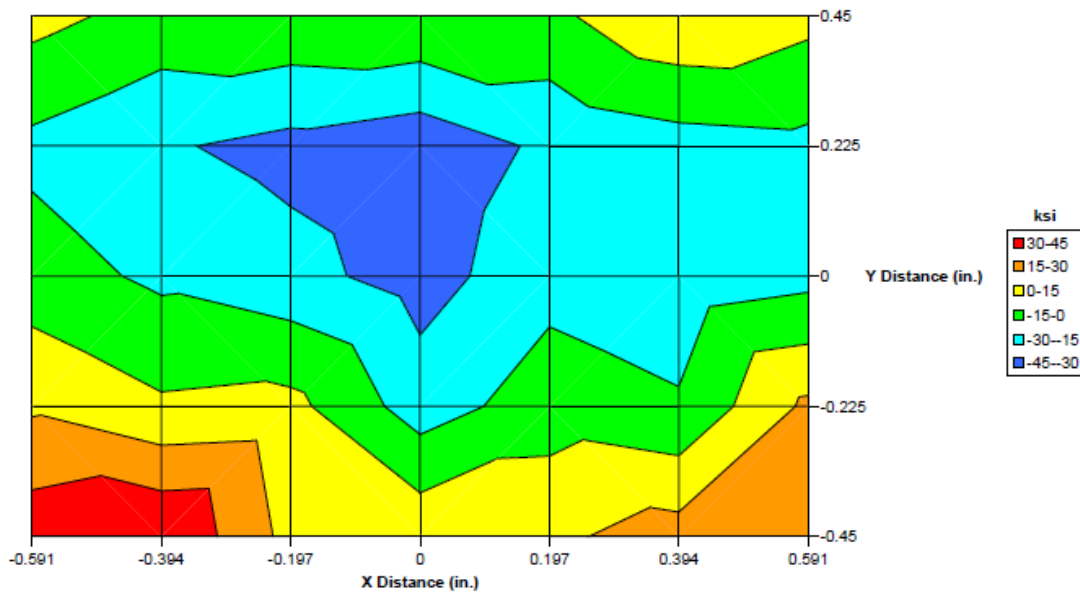


Figure 2.6 Example of residual stress profile at the 316SS-316SS plate weld cross-section.

3.5 Conclusions

In this brief summary report, the ongoing research activities related to both mechanistic modeling and experimental activities are summarized with some representative examples. The results shown are preliminary in nature and not complete and hence no firm conclusions can be drawn.